

Dynamics of the BCS-BEC crossover in a degenerate Fermi gas

M. H. Szymańska¹, B. D. Simons¹, and K. Burnett²

¹ *Cavendish Laboratory, University of Cambridge, Madingley Road, Cambridge CB3 0HE, UK*

² *Clarendon Laboratory, University of Oxford, Parks Road, Oxford, OX1 3PU, UK*

We study the short-time dynamics of a degenerate Fermi gas positioned near a Feshbach resonance following an abrupt jump in the atomic interaction resulting from a change of external magnetic field. We investigate the dynamics of the condensate order parameter and pair wavefunction for a range of field strengths. When the abrupt jump is sufficient to span the BCS to BEC crossover, we show that the rigidity of the momentum distribution precludes any atom-molecule oscillations in the entrance channel dominated resonances observed in the ⁴⁰K and ⁶Li. Focusing on material parameters tailored to the ⁴⁰K Feshbach resonance system at 202.1 gauss, we comment on the integrity of the fast sweep projection technique as a vehicle to explore the condensed phase in the crossover region.

PACS numbers: 03.75.Kk, 03.75.Ss, 05.30.Fk

Ultracold alkali atomic gases provide a valuable arena in which to explore molecular Bose-Einstein condensation (BEC) [1] and fermionic pair condensation [2, 3]. Further, the facility to control interparticle interactions via a magnetically-tuned Feshbach resonance (FR) provide a unique opportunity to investigate the BCS-BEC crossover and the dynamics of condensate formation. As well as the adiabatic association of molecules [1], both fast sweep ‘projections’ of fermionic pair condensates onto the molecular BEC [2, 3], and atom-molecule Ramsey fringes [4] have been reported in the recent literature. Lately, motivated by earlier work on the mean-field BCS system [5], it was shown in separate works [6, 7] that the mean-field equations of motion of a Bose-Fermi (BF) model, commonly used to describe the FR system, are characterised by an integrable nonlinear dynamics. From these works, three striking predictions emerged: Firstly, when perturbed by an abrupt change in the strength of the pair interaction, the condensate order parameter exhibits substantial oscillations which range in magnitude between some initial state value, Δ_I , and that expected for the equilibrium final state configuration Δ_{eq} . Secondly, in the absence of energy relaxation processes, these oscillations remain undamped suggesting the potential to observe coherent atom-molecule oscillations in the FR system. Thirdly, it is proposed that a spectral ‘hole-burning’ phenomena in the atomic momentum distribution, at a frequency associated with one half of the molecular binding energy, provides a signature of such atom-molecule oscillations [7].

In the following, we will argue that this behaviour rests on an auxiliary constraint that, in the present system, seems hard to justify. Drawing on the results of a numerical analysis of the unconstrained dynamics, we will show that, in the absence of relaxational processes, the oscillations of the order parameter are damped substantially, even at the level of the mean-field. When the abrupt change of the interaction is sufficient to span the BCS-BEC crossover, for both the single channel and BF systems, the magnitude of oscillations remain small attenuating to some value Δ_F which lies close to the initial

state, and much smaller than the expected equilibrium state value, Δ_{eq} , while the distribution remains essentially “frozen” to the initial state. The hole-burning oscillations of the form predicted in Ref. [7] do not appear in either regime. From these results, we are able to conclude that, although the observation of BCS-BEC like atom-molecule oscillations in alkali Fermi gases seems infeasible, the rigidity of the initial state distributions validate fast sweep techniques [2] as a reliable experimental tool to explore the crossover region.

Formally, a detailed microscopic theory of FR phenomena demands consideration of all matrix elements connecting different spin states participating in condensate formation. In practice, an accurate description of the resonance can be obtained either by using a single-channel magnetic field dependent effective interaction between atoms in the entrance channel or, more widely, in the two-most relevant channels. For low relative momenta, relevant to cold atom physics, the full form of complex atomic potentials are not resolved. Indeed, separable potentials with microscopic parameters drawn from experiment and exact multichannel calculations can be used to recover all low-energy binary scattering observables [10, 11]. Since, very often, only one bound state of the closed channel potential is relevant, it has been traditionally replaced by a fictitious Bose-particle and FR phenomena captured by an effective two-channel BF Hamiltonian [12, 13].

Now, applied to the entrance channel dominated resonances observed in the ⁴⁰K and ⁶Li system, formal calculations [10, 11] support a picture in which the BCS-BEC crossover *is mediated by only a very small admixture of closed channel states* — e.g., in the ⁴⁰K FR at 202.1 gauss, the admixture of the closed channel is ca. 8% or less of the total [11]. Rather, the weakly bound molecular state appears at a detuning E_0 which lies far from the value where the resonance state of the closed channel crosses the dissociation threshold. Since the two-body observables drawn from the exact numerical solution of the Schrödinger equation within finite-range single and two-channel models do not differ over a wide range of fields [11], FR phenomena in ⁴⁰K can be equally-well de-

scribed by a single-channel theory,

$$\hat{H} = \sum_{\mathbf{k}s} \epsilon_{\mathbf{k}} a_{\mathbf{k}s}^\dagger a_{\mathbf{k}s} + \sum_{\mathbf{k}\mathbf{k}'\mathbf{q}} V_{\mathbf{k}\mathbf{k}'} a_{\mathbf{k}+\mathbf{q}\uparrow}^\dagger a_{-\mathbf{k}\downarrow}^\dagger a_{-\mathbf{k}'\downarrow} a_{\mathbf{k}'+\mathbf{q}\uparrow}, \quad (1)$$

involving Fermi operators $a_{\mathbf{k}s}^\dagger$ and $a_{\mathbf{k}s}$. In the following, to account for the entire region of crossover (and not only the universal regime) we take as matrix elements $V_{\mathbf{k}\mathbf{k}'} = V_0(B)\chi_{\mathbf{k}}(\sigma_{\text{bg}})\chi_{\mathbf{k}'}(\sigma_{\text{bg}})$ with $\chi_{\mathbf{k}}(\sigma_{\text{bg}}) = \exp[-(\mathbf{k}\sigma_{\text{bg}})^2/2]$ and the parameters $V_0(B)$ and σ_{bg} chosen to recover the correct magnetic field dependence of the scattering length and the highest vibrational bound state [11].

Applied to the fields $\Phi_{\mathbf{k}} = \sum_s \langle a_{\mathbf{k}s}^\dagger a_{\mathbf{k}s} \rangle / 2$ and $\kappa_{\mathbf{k}} = \langle a_{-\mathbf{k}\downarrow} a_{\mathbf{k}\uparrow} \rangle$, the Heisenberg equations of motion $i\langle \dot{A} \rangle = \langle [A, \hat{H}] \rangle$ translate to the relations

$$\begin{aligned} i\dot{\kappa}_{\mathbf{k}} &= 2\epsilon_{\mathbf{k}}\kappa_{\mathbf{k}} - \Delta_{\mathbf{k}}(2\Phi_{\mathbf{k}} - 1) \\ i\dot{\Phi}_{\mathbf{k}} &= \Delta_{\mathbf{k}}\kappa_{\mathbf{k}}^* - \Delta_{\mathbf{k}}^*\kappa_{\mathbf{k}}, \end{aligned} \quad (2)$$

where $\Delta_{\mathbf{k}} = V_0(B)\chi_{\mathbf{k}}(\sigma_{\text{bg}})\sum_{\mathbf{k}'}\chi_{\mathbf{k}'}(\sigma_{\text{bg}})\kappa_{\mathbf{k}'}$ denotes the complex order parameter. Similarly for a BF theory, defining $g_{\mathbf{k}} = g_0\chi_{\mathbf{k}}(\sigma)$ as the coupling of the entrance channel states to the bosonic field $b_{\mathbf{k}}$ associated with the Feshbach resonance level configuration of the closed channel, the equations of motion acquire the same form as (2) with $\Delta_{\mathbf{k}} = g_0\chi_{\mathbf{k}}(\sigma)b_0 + V_{\text{bg}}\chi_{\mathbf{k}}(\sigma_{\text{bg}})\sum_{\mathbf{k}'}\chi_{\mathbf{k}'}(\sigma_{\text{bg}})\kappa_{\mathbf{k}'}$ and $b_0 = \langle b_{\mathbf{k}=0} \rangle$ obeying the supplementary equation $i\dot{b}_0 = E_0(B)b_0 + g_0\sum_{\mathbf{k}}\chi_{\mathbf{k}}(\sigma)\kappa_{\mathbf{k}}$. As with the single-channel theory, the five parameters which characterise the resonance, the background potential strength V_{bg} and range σ_{bg} (which define the entrance channel scattering length and its highest vibrational bound state), the interchannel coupling g_0 and its range σ , and the detuning $E_0(B)$ (which specifies the position and width of the resonance), are determined from experiment and exact multichannel calculations [11].

Before turning to the numerical analysis, it is instructive to contrast the present approach to that adopted in Refs. [5, 6, 7]. Given an initial condition, the Heisenberg equations of motion (2) present a deterministic time evolution of the density distributions. Indeed, the conservation of total atomic density n , implicit in the dynamics (2), provides a check on the integrity of the numerical integration described below. By contrast, the integrability of the equations of motion as described by Refs. [5, 6, 7] relies on an additional constraint involving the density and an auxiliary parameter playing the role of a “chemical potential”. The need for this constraint originates from the fact that, as with the equilibrium steady state solution, the analytical solution of the dynamical equations is determined only up to an arbitrary momentum dependent sign factor which is fixed by the auxiliary constraint [7], instead of naturally following from the initial conditions. A similar phenomenology describes the effect of a classical laser source on a semiconductor electron/hole system where the laser frequency “imprints” a chemical potential onto the system [9]. While equilibration processes are sufficiently small, the electrons and

holes assume a non-equilibrium distribution around the externally imposed chemical potential resulting in a phenomenon of “spectral-hole burning” in which the density distribution is depleted at the laser frequency. In the atomic gas system, where the degrees of freedom remain internal, it is difficult to see how such a choice is motivated or justified. Crucially, we will see that the unconstrained dynamics associated with the equations of motion (2) lead to physical behaviour very different from that obtained from the constrained dynamics [5, 6, 7].

With this background, let us now turn to the results of the numerical investigation of the dynamics (2) performed using an adaptive step Runge-Kutta algorithm applied on a grid in momentum space chosen fine enough to ensure convergence at each time step. Although we find that the qualitative behaviour of BCS and BF dynamics is generic, we focus specifically on potentials characteristic for the ^{40}K resonance at $B_0 = 202.1$ gauss with a density of $n = 1.5 \times 10^{13} \text{ cm}^{-3}$ (i.e. $T_F = 0.35 \mu\text{K}$) comparable to that used in experiment [2]. With these parameters, the equilibrium properties of the effective single-channel and BF model essentially coincide (for further details and values of parameters, we refer to Ref. [11]). Therefore, to keep our discussion concise, we will focus on the single-channel theory noting that the parallel application to the BF model with appropriate physical parameters generates *quantitatively* similar results. At a field of ca. 1.0 gauss above the FR, the

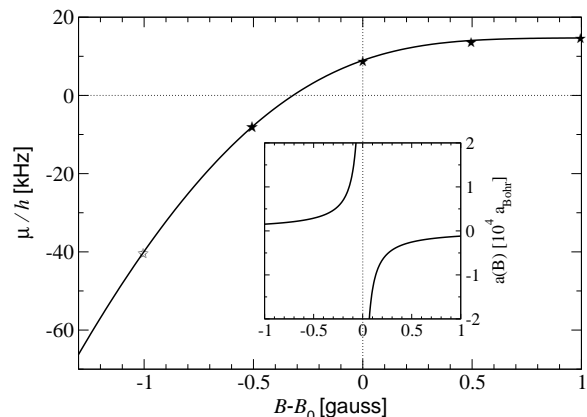


FIG. 1: Variation of the chemical potential μ with field B at $T = 0$ for a mixture of fermionic ^{40}K atoms prepared in the ($f = 9/2, m_f = -9/2$) and ($f = 9/2, m_f = -7/2$) Zeeman states at a density of $n = 1.5 \times 10^{13} \text{ cm}^{-3}$ (i.e. $T_F = 0.35 \mu\text{K}$). The FR takes place at a field $B_0 = 202.1$ gauss while the BEC-BCS crossover ($\mu = 0$) occurs when $B - B_0 \simeq 0.3$ gauss. The inset indicates the scattering length $a(B) = a_{\text{bg}}(1 - \frac{\Delta B}{B - B_0})$ in the universal regime, where a_{bg} is the background potential scattering length and ΔB the width of the resonance. Note that, in the present theory, we use finite range potentials with parameters which describe the FR also far outside the universal region [11].

condensate has an essentially BCS-like character while the experiment using the fast sweep technique observed the condensate starting from 0.5 gauss above B_0 . To ex-

plore the entire region of interest, we choose as initial conditions field values B_I which span the entire crossover region (marked by stars in Fig. 1). Starting from the ground state $T = 0$ distribution, we follow the dynamics of the condensate after an abrupt switch to some different value of magnetic field B_F .

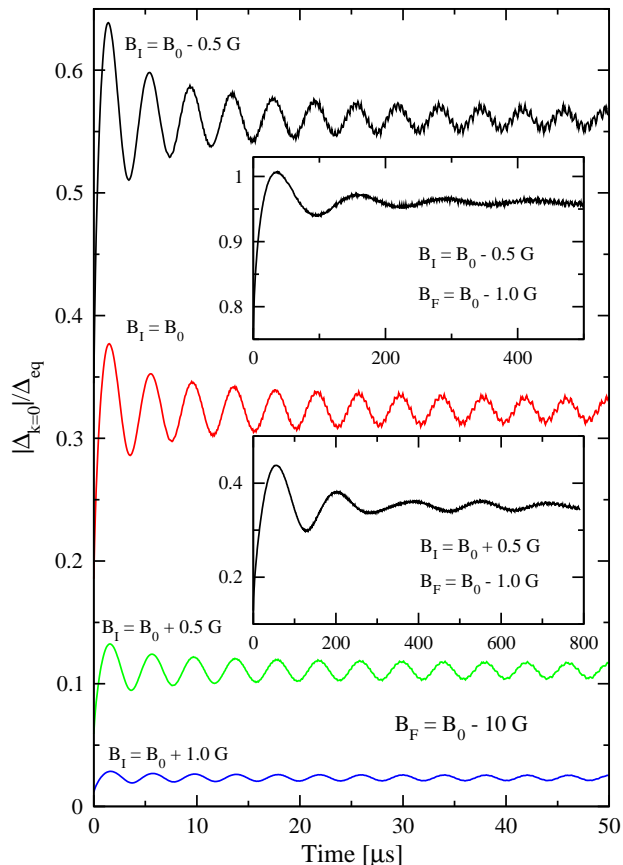


FIG. 2: Time dependence of the order parameter amplitude $|\Delta_{\mathbf{k}=0}|/\Delta_{\text{eq}}$ following an abrupt switch from a field of $(B_I - B_0)/\text{gauss} = -0.5$ (top), 0.0, 0.5, 1.0 (bottom) to $(B_F - B_0)/\text{gauss} = -10$, and from $(B_I - B_0)/\text{gauss} = -0.5$ (top inset) and $(B_I - B_0)/\text{gauss} = 0.5$ (bottom inset) to $(B_F - B_0)/\text{gauss} = -1.0$. In addition to the constant phase velocity of $\Delta_{\mathbf{k}=0}$ (found numerically to be set by the final state equilibrium chemical potential μ), there is an additional time-dependent phase modulation whose characteristics mirror closely that of the amplitude oscillations.

Figure 2 shows the time-evolution of the order parameter $|\Delta_{\mathbf{k}=0}|$, normalised by the value, Δ_{eq} (i.e. the value that it would acquire were the system to reach the $T = 0$ ground state at the final field B_F). Here we have chosen a field $B_F - B_0 = -10$ gauss deep within the BEC phase where the large binding energy of molecules allows their momentum distribution to be inferred from time of flight measurements [2]. In contrast to the predictions of the constrained dynamics [5, 6, 7], these results show that (a) the coherent oscillations are substantially damped even at the level of mean-field, (b) the amplitude of the oscillations is small, and (c) the order parameter $|\Delta_{\mathbf{k}=0}|$

asymptotes to a value much less than the expected final state equilibrium value Δ_{eq} . Referring to the insets of Fig. 2, one may note that, when the initial and final conditions are drawn closer, the period of the oscillations becomes longer and the effects of the damping more pronounced. Moreover, although the period of the oscillations increases monotonically with Δ_{eq} , the dependence is nonlinear and, referring to the bottom inset of Fig. 3, one may note that Δ_{eq} does not provide a ceiling for the magnitude of the oscillation.

To interpret the generic behaviour, it is instructive to access the time-dependence of the pair wavefunction $\kappa_{\mathbf{k}}$ and the distribution function $\Phi_{\mathbf{k}}$. Figure 3 shows that, when the abrupt switch takes place from $B_I - B_0 = 0.5$ gauss to $B_F - B_0 = -10$ gauss, although there is a slight tendency to shift towards the final state equilibrium distribution, the pair wavefunction and the density distribution remain essentially frozen close to the initial BCS-like distribution, exhibiting only small oscillations in time. In the absence of energy relaxational processes, the system is unable to significantly redistribute weight. By contrast, when the abrupt switch takes place from $B_I - B_0 = 0.5$ gauss to $B_F - B_0 = -1.0$ gauss, the proximity of the two phases allows the system to converge to a (non-stationary) modulated distribution whose (stationary) envelope reflects more closely the final state equilibrium distribution. Referring to insets in the bottom panel one may note that a weakly perturbed condensate on the BCS side attenuates to its equilibrium value with the pair distribution showing only small modulations around the equilibrium in accord with the linear stability analysis of the weakly perturbed BCS system (2) discussed in Ref. [15]. In particular, one may note that here (and, indeed, for other values of the initial and final conditions) the hole-burning phenomenon predicted by the constrained dynamics [7] does not appear.

To assess the potential to observe coherent atom-molecule oscillations, one can monitor the time evolution of the number of condensed molecules,

$$n_{\text{mc}}(t) = \left| \int d^3k \kappa_{\mathbf{k}}(t) \phi_{\text{B}}(k, B_F) \right|^2. \quad (3)$$

Here $\phi_{\text{B}}(k, B_F)$ denotes the wavefunction of the highest vibrational bound state being an exact eigenstate of the two-body problem [11]. Referring to Fig. 4, one may note that the amplitude of oscillations is negligible (less than one percent). Although one may adjust the final field B_F to lie closer to the FR, the amplitude of the oscillations increases only slightly while the damping rate is also enhanced. Moreover, the inclusion of processes beyond the mean-field approximation considered here would simply increase the damping rate and not enhance the oscillations. One may therefore conclude that the observation of atom-molecule oscillations, following an abrupt change in the interaction strength, is infeasible for the entrance channel dominated resonances currently discussed in the context of the ^{40}K and ^6Li system.

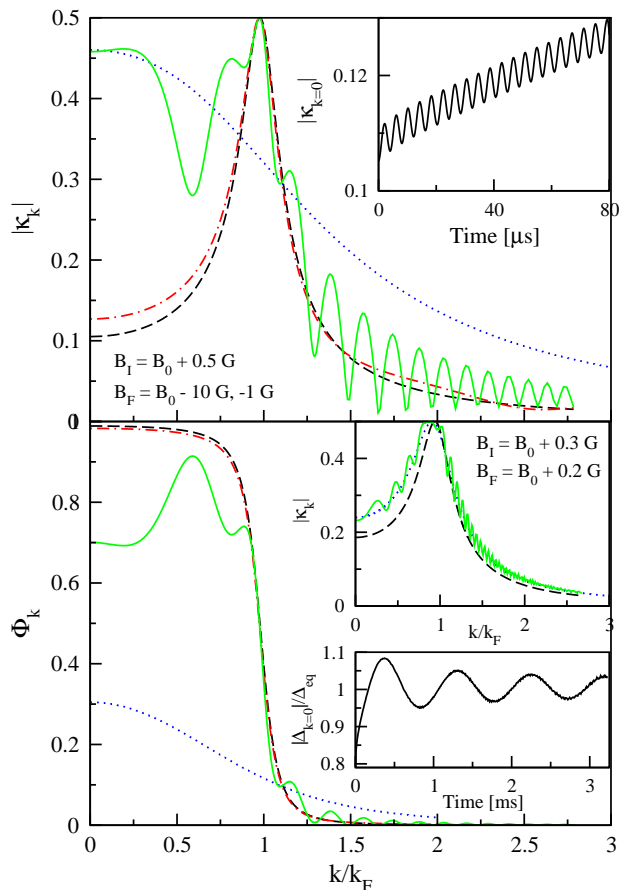


FIG. 3: The pair wave-function $|\kappa_{\mathbf{k}}|$ (upper panel) and the density distribution function $\Phi_{\mathbf{k}}$ (lower panel) shown as function of $k = |\mathbf{k}|$ with $B_I - B_0 = 0.5$ gauss (dashed lines) and $B_F - B_0 = -10$ gauss after $50 \mu\text{s}$ (dashed-dotted line) and $B_F - B_0 = -1.0$ gauss after $800 \mu\text{s}$ (solid line) following the abrupt switch as in Fig. 2. The dotted lines signify the ground state equilibrium distributions at $B_F - B_0 = -1.0$ gauss included for comparison. The upper inset shows oscillations of $|\kappa_{\mathbf{k}=0}|$ for $B_F - B_0 = -10$ gauss. The lower two insets refer to a rather weak perturbation on the BCS side from $B_I - B_0 = 0.3$ gauss (dashed line) to $B_F - B_0 = 0.2$ gauss. The dotted lines shows the equilibrium distribution while the solid line provides a snap-shot of the distribution at 3 ms after the switch. Note that the harmonic modulations visible in the distribution functions translate to a single energy scale of the same order of magnitude as the period of oscillations seen in $|\Delta_{\mathbf{k}=0}|$.

To conclude, we have presented a numerical analysis of the dynamical mean-field equations for the single-channel theory of the FR following an abrupt field change. In the range of physical parameters appropriate to the ^{40}K system, the consideration of the two-channel BF (Bose-Fermi) theory does not change the results *quantitatively*. When applied to a theoretical regime where the pop-

ulation of the closed channel states below resonance is high, the numerical findings do not change *qualitatively*. Relying on the deterministic time-evolution of the initial state according to the Heisenberg mean-field equa-

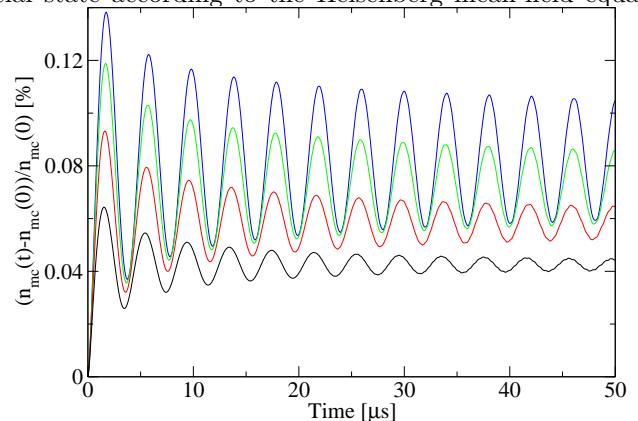


FIG. 4: Time-dependence of the relative number of condensed molecules $(n_{\text{mc}}(t) - n_{\text{mc}}(0))/n_{\text{mc}}(0)$. Here we have used the same field values as that used in Fig. 2 (main) with $(B_I - B_0)/\text{gauss} = -0.5$ (top), 0.0, 0.5, and 1.0 (bottom) and $(B_F - B_0)/\text{gauss} = -10$. For these field values, when normalised to one half of the total atomic density, $n_{\text{mc}}(0) = 0.0005, 0.012, 0.1, \text{ and } 0.3$ respectively.

tions of motion, our results differ substantially from the findings of the constrained dynamics considered previously [5, 6, 7]. Over a wide range of initial conditions, we observe substantially damped oscillations with an amplitude strongly dependent on initial conditions and a frequency set by the interaction strength after the switch. To assess the capacity for BCS-BEC like atom-molecule oscillations following an abrupt change in the interaction, we have chosen initial and final conditions to span the crossover from the BCS to the BEC limits. We have found that the amplitude of atom-molecule oscillations is negligible and the distribution is essentially frozen to the initial, a behaviour reminiscent of an orthogonality catastrophe. We conclude that, in the entrance channel dominated resonances observed in ^{40}K and ^6Li , the observation of atom-molecule oscillations is infeasible. The rigidity of the condensate wavefunction distribution at short-time scales, where the time evolution is mean-field in character, supports the method of the fast sweep as a reliable technique to probe the fermionic pair condensate.

We are grateful to Krzysztof Góral and Thorsten Köhler for numerous discussions concerning the FR physics, to Peter Littlewood for stimulating discussions and to Sławomir Matyjaśkiewicz for advice concerning the numerical techniques. This research has been supported by Gonville and Caius College Cambridge (M.H.S.)

[1] M. Greiner, *et al.*, Nature **426**, 537 (2003); S. Jochim, *et al.*, Science, **302**, 2102 (2003); M. W. Zwierlein, *et al.*,

Phys. Rev. Lett. **91**, 250401 (2003).

- [2] C. A. Regal, *et al.*, Phys. Rev. Lett. **92**, 040403 (2004).
- [3] M. W. Zwierlein, *et al.*, Phys. Rev. Lett. **92**, 120403 (2004).
- [4] E. A. Donley, *et al.*, Nature **417**, 529 (2002).
- [5] R. A. Barankov, *et al.*, Phys. Rev. Lett. **93**, 160401 (2004).
- [6] R. A. Barankov, *et al.*, Phys. Rev. Lett. **93**, 130403 (2004).
- [7] A. V. Andreev, *et al.*, Phys. Rev. Lett. **93**, 130402 (2004).
- [8] E. A. Yuzbashyan, *et al.*, cond-mat/0407501.
- [9] S. Schmitt-Rink, *et al.* Phys. Rev. B **37**, 941-955 (1988).
- [10] K. Góral, *et al.*, J. Phys. B **37**, 3457 (2004).
- [11] M. H. Szymańska, K. Góral, T. Köhler, K. Burnett, unpublished
- [12] M. Holland, *et al.*, Phys. Rev. Lett. **87**, 120406 (2001); E. Timmermans, *et al.*, Phys. Lett. A **285**, 228 (2001); Y. Ohashi, *et al.*, Phys. Rev. Lett. **89**, 130402 (2002).
- [13] Note that the particular architecture of the hyperfine states in the ^{40}K system calls into question the validity of a BF model as a microscopic theory [14].
- [14] M. M. Parish, *et al.*, cond-mat/0409756 (2004).
- [15] A. F. Volkov and Sh. M. Kogan, Sov. Phys. JETP, **38**, 1018 (1974).